

Comparison of simulation results of ENSO and IOD using the climate model SPEEDY with ERA5 and NCEP reanalysis data

Aydin, Onurhan

Knop, Irmgard

Schubert, Natalie

Wolter, Ole

Johann Wolfgang Goethe Universität Frankfurt am Main

2025-02-17

Abstract: Research has improved the understanding of the occurrence and global impacts of the ENSO and the IOD cycle. However, this is made more difficult as the global climate is changing. To determine the accuracy and reliability of the SPEEDY model, results were compared to observational and reanalysis data. The model has been run over the time span of six months for two different climate patterns: the ENSO cycle (El Niño and La Niña) and the IOD cycle (IOD+ and IOD-). The sea surface temperature, the precipitation and the zonal and meridional wind for the corresponding area were examined of the ENSO cycle and the IOD cycle. While SPEEDY was able to reproduce the ENSO events well qualitatively, it was found to struggle to recreate the IOD events, most notably regarding the atmospheric circulation.

Contents

1	Introduction	3
2	Idealized cases	3
2.1	El Niño	3
2.2	La Niña	4
2.3	IOD+	5
2.4	IOD-	6
3	SPEEDY setup and reanalysis datasets	7
4	Results and Discussion	7
4.1	El Niño	7
4.1.1	Sea surface temperature	7
4.1.2	Precipitation	10
4.1.3	Wind and Circulation	12
4.2	La Niña	14
4.2.1	Sea surface temperature	14
4.2.2	Precipitation	16
4.2.3	Wind and Circulation	18
4.3	IOD+	19
4.3.1	Sea surface temperature	19
4.3.2	Precipitation	21
4.3.3	Wind and Circulation	23
4.4	IOD-	25
4.4.1	Sea Surface Temperature	25
4.4.2	Precipitation	26
4.4.3	Wind Circulation	28
5	Conclusion and outlook	29

1 Introduction

With global warming and climate change receiving more attention, it is required that models are able to correctly forecast regional circulation systems influencing the climate on a global scale. One of such climate models is the SPEEDY (Simplified Parameterizations, primitE-Equation DYnamcs) model. Developed at the International Centre for Theoretical Physics (ICTP) in Castello di Miramare, Italy, it is used in recent times e. g. to assess the influence of ENSO patterns on droughts over southern Africa ([Gore et al. 2020](#)), to investigate the global and regional climatic impacts of Modoki-ENSO circulation ([Dogar et al. 2019](#)) or in a paper analyzing the Arctic Oscillation and North Atlantic Oscillation decoupling in a case of a warmer climate ([Hamouda et al. 2021](#)). In order to determine the accuracy and reliability of the model, results must be compared to verified climate data, for example observational or reanalysis data. In order to analyze the global or regional effects of the ENSO cycle (consisting of El Niño and La Niña events) and the IOD cycle (consisting of IOD+ and IOD-) using SPEEDY, one must first determine to what extent SPEEDY is able to simulate these climate events accurately. Therefore, in this report, the sea surface temperature (SST), precipitation, and winds during these four climate events are analyzed. The focus is on the regions, where the events primarily occur. We start in section 2 by discussing the course and influence of El Niño , La Niña, IOD+, and IOD-. In section 3 we describe how SPEEDY was set up and what reanalysis and observational data was used for the later comparisons. The results for each climate event are given and discussed in section 4. We end the report with a conclusion and an outlook, which can be found in section 5.

2 Idealized cases

2.1 El Niño

During an El Niño event, an elevated sea surface temperature near the equator in the Pacific Ocean causes an increase in rainfall, as is illustrated in fig. 1. These temperature anomalies further influence e.g. the hurricane occurrences in America. However, this will not be discussed in the report.

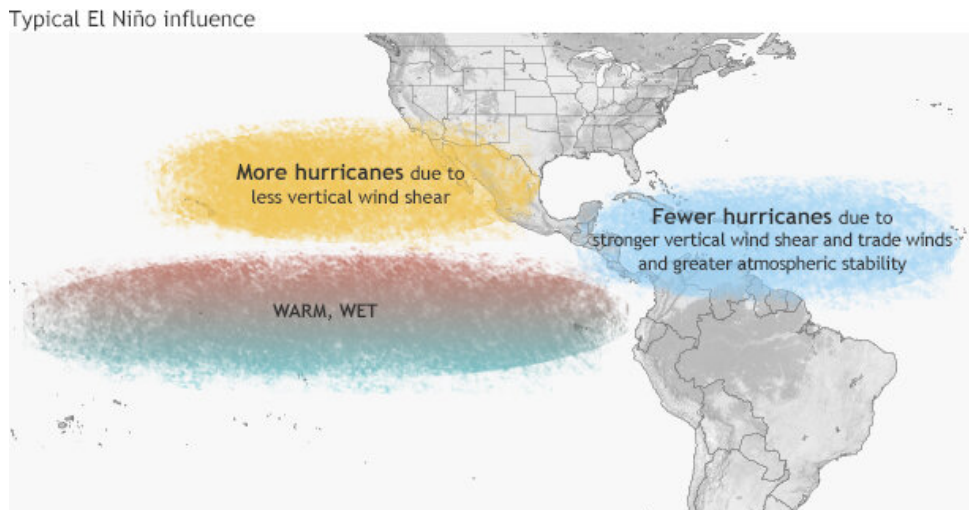


Figure 1: Typical El Niño influence regarding the sea surface temperature, the hurricane frequency, and the precipitation in the east Pacific and America ([NOAA 2021](#)).

The increase in precipitation over the Pacific is due to a change in winds over the region. Weakened trade winds allow for more convection in the El Niño region, resulting in higher

precipitation, as can be seen in fig. 2

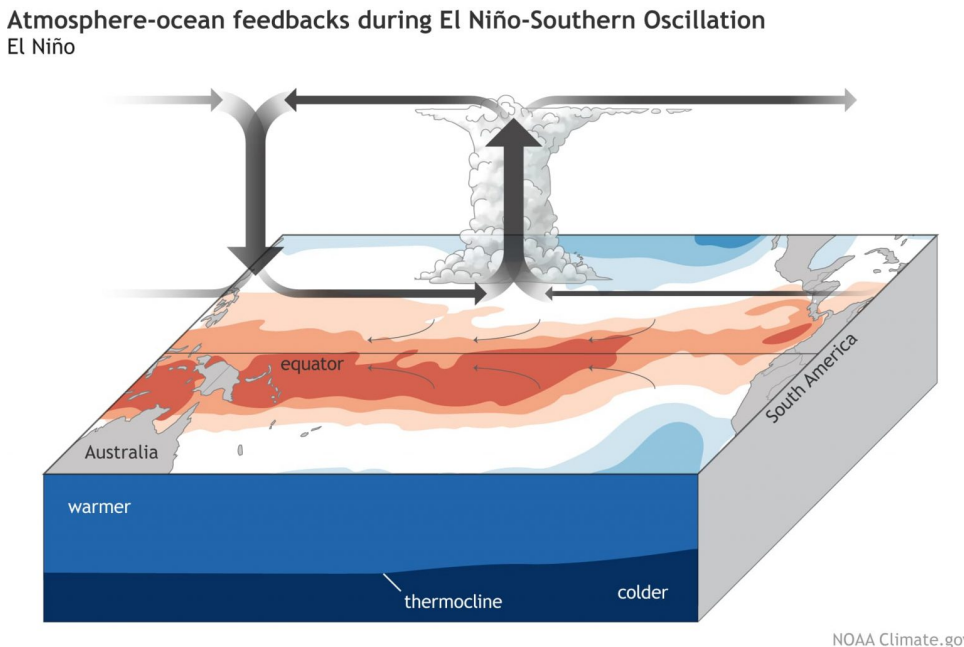


Figure 2: Typical El Niño influence regarding the sea surface temperature and air circulation over the Pacific ([Snowbrains 2020](#)).

2.2 La Niña

Figure 3 shows the typical situation in the case of a La Niña event focusing on the sea surface temperatures, the precipitation in the east Pacific and the hurricane frequency over middle America, which is in general not discussed in this report. It can be seen that the sea surface

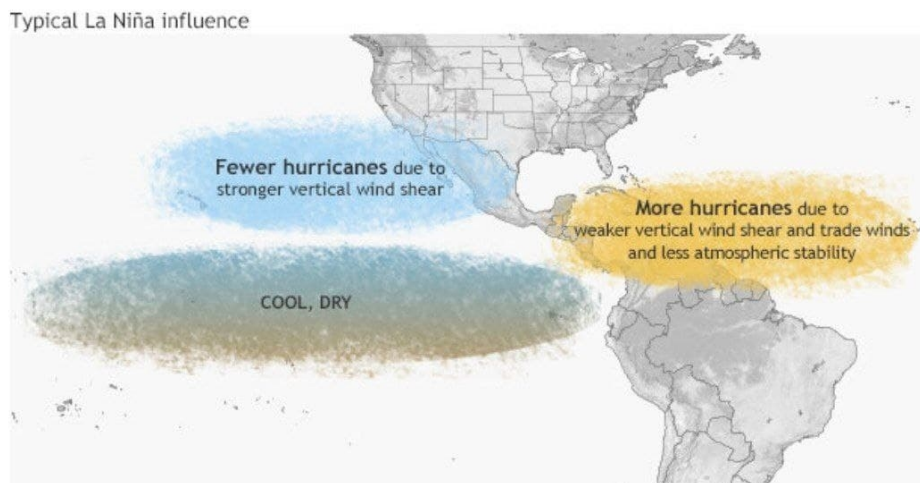
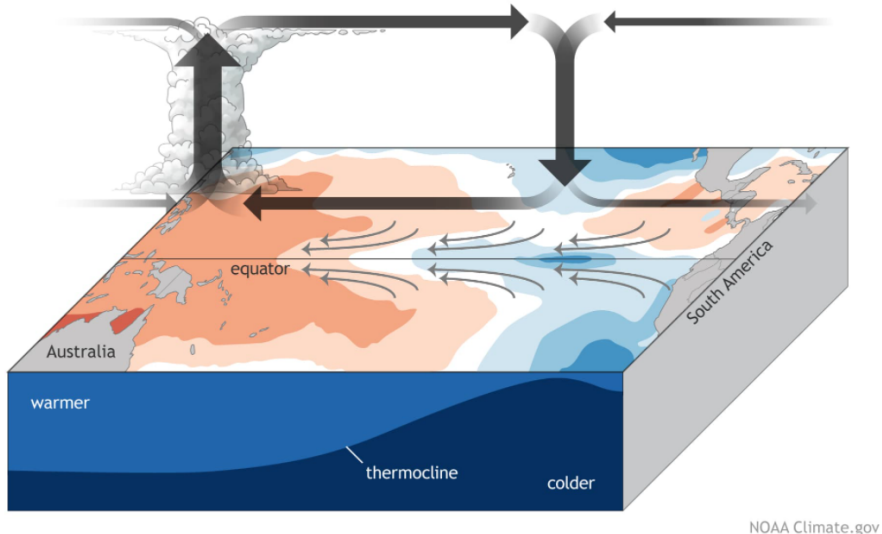


Figure 3: Typical La Niña influence regarding the sea surface temperature and the hurricane frequency in the east Pacific and America ([NOAA 2021](#)).

in the east Pacific is colder than usual in the case of a La Niña event and that there is less precipitation in this area.

Figure 4 shows the wind behavior during a La Niña event. In the equatorial region over the Pacific there is east wind coming from America. Above Indonesia the air then rises leading to



NOAA Climate.gov

Figure 4: Typical La Niña influence regarding the sea surface temperature and the wind pattern over the Pacific ([Snowbrains 2020](#)).

cloud formation and possibly more precipitation in this region. The air is then moving to the east again, where it sinks above the Pacific ocean. This report focuses only on the surface near winds, which means that the interesting area in the picture is over the Pacific where east wind is shown. Figure 4 also illustrates the sea surface temperatures again. The east Pacific is cold during a La Niña event, whereas the west Pacific is warmer.

2.3 IOD+

The positive phase of the Indian Ocean Dipole Circulation features an alteration of the sea surface temperature distribution in the Indian Ocean. While the water is warmer than usual in the western part, the water temperature is cooler than usual in the eastern part of the Indian Ocean. This leads to a change in the Walker cell circulation in such a way that easterly instead of westerly winds are then present over the equatorial Indian Ocean. This reversal in respect to the normal state enhances the convection over the Horn of Africa which goes along with higher precipitation in that region. Simultaneously, the convection is reduced over the eastern Pacific leading to less precipitation than usual and in extreme cases to droughts ([World Climate Service 2021](#)). The described scheme is visualized in the following graphic 5

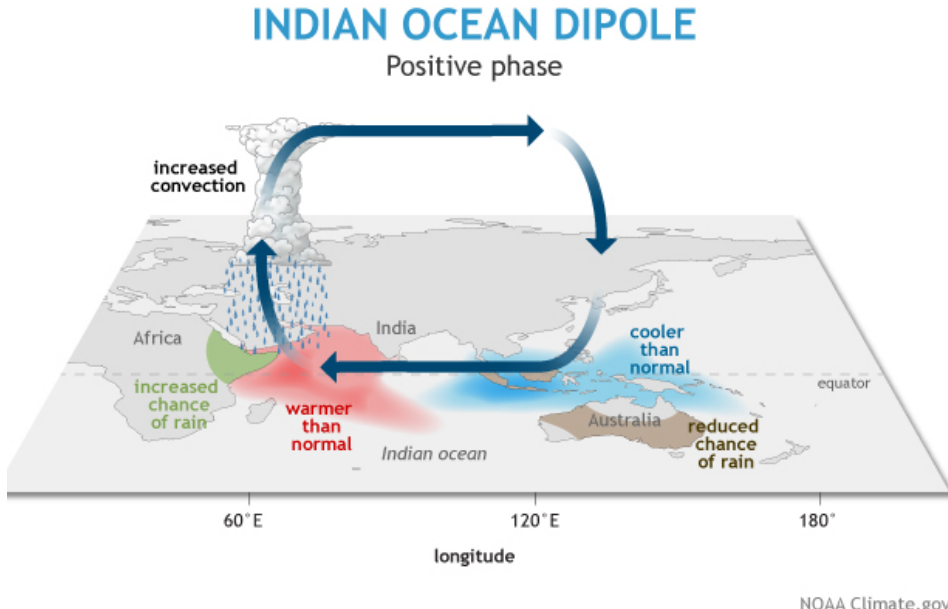


Figure 5: Schematic graphic of the Indian Ocean Dipole’s positive phase ([World Climate Service 2021](#)).

2.4 IOD-

A negative IOD event is characterized by warmer than normal water in the tropical eastern Indian Ocean and colder than normal water in the tropical western Indian Ocean [1]. This is associated with the condition that the normal convection situated over the western Indian Ocean warm pool shifts to the east and brings heavy rainfall over the Indonesia and Australia and this also could lead to droughts over the east Africa and Sri Lanka. Additionally, recent studies show that IOD events clearly impact climate parameters that will be evaluated in the paper in the dry season. The anomalous atmospheric circulation may trigger planetary atmospheric waves, by which the IOD also influences global climate [4]. In the last two decades, IOD has attracted much attention because of its climate impacts in the Indian Ocean rim and other regions [5]. Accuracy of SPEEDY showed its efficiency by comparing with reanalysis and observational data.

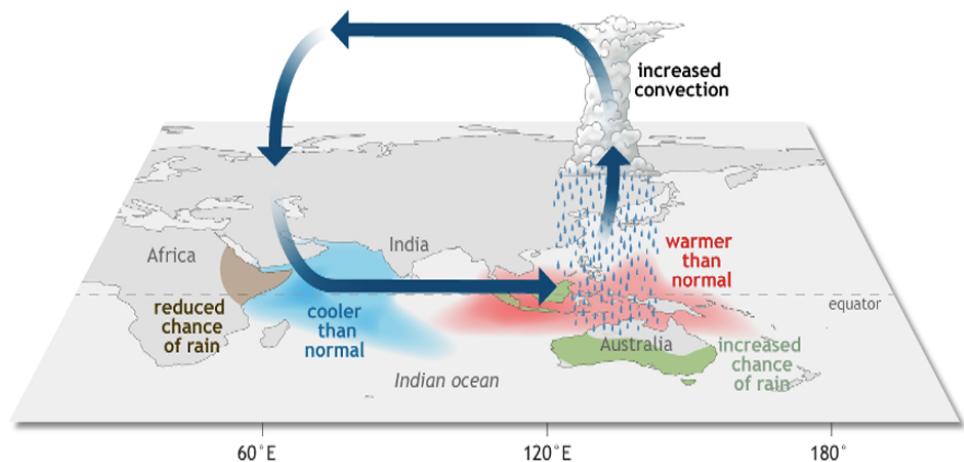


Figure 6: The general aspect of the atmospheric circulation during the negative IOD event ([World Climate Service 2021](#)).

3 SPEEDY setup and reanalysis datasets

The model has been set up to run over a six month time span. For the individual climate event, the following time periods where used:

El Niño : January 2016 - June 2016

La Niña: July 2016 - December 2016

IOD+: June 2015 - November 2015

IOD-: July 2013 - December 2013

The runs use the following sea surface temperature (SST) anomalies:

El Niño : `sst_composite_nino34_p1.grd`

La Niña: `sst_composite_nino34_m1.grd`

IOD+: `sst_composite_iod_p1.grd`

IOD-: `sst_composite_iod_m1.grd`

Although there are various climatological parameters that are simulated, sea surface temperature, precipitation and meridional and zonal winds were analyzed in this paper. The simulated data was compared to reanalysis data obtained from the Climate Data Store by Copernicus using a ERA5 data set ([Copernicus 2019](#)) and a NCEP data set obtained from the NOAA Physical Sciences Laboratory ([NOAA 2022c](#)). The ERA5 sea surface temperature and precipitation data was compared to observational data also obtained from the NOAA Physical Sciences Laboratory ([NOAA 2022a,b](#)). The influences were assessed over the area between $\pm 40^{\circ}\text{N}$ in the case of El Niño and La Niña. The analyzed region for IOD+ and IOD- is $\pm 40^{\circ}\text{N}$ and 35 to 160°E .

4 Results and Discussion

In the following, the SPEEDY results are compared to ERA5 and NCEP reanalysis data. ERA5 data is partially compared to observational data.

4.1 El Niño

4.1.1 Sea surface temperature

In order to determine if ERA5 provides accurate SST data, we compare it to observational data. The difference between the mean SST given by ERA5 and the mean observed SST from January to June 2016 are illustrated in fig. 7. In the El Niño region, the anomalies are at most 0.6 K, however usually between -0.3 K and 0.3 K . Further away from the El Niño region, there are regions with higher anomalies, e.g. the Atlantic Ocean near the equator, between South America and Africa. Yet, as the focus is on the El Niño region, we can conclude that ERA5 sufficiently represents the SST from January to June 2016.

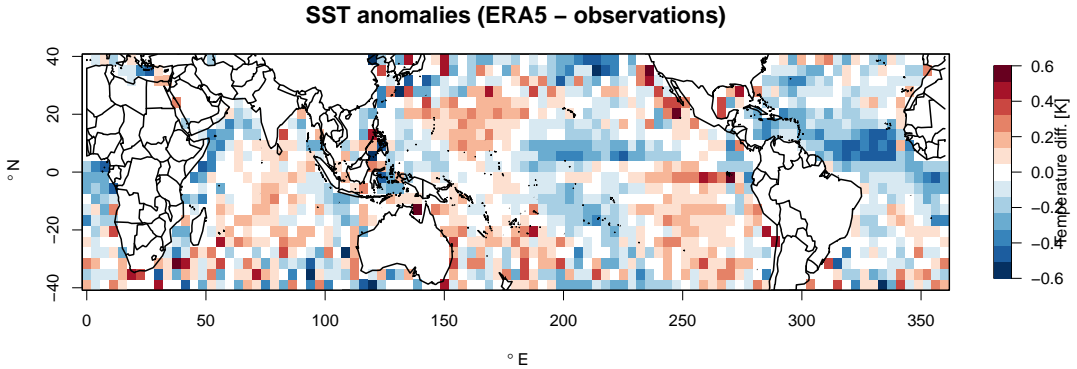


Figure 7: Mean SST anomalies of ERA5 compared to observational data.

Furthermore, we must verify that the SST in SPEEDY and ERA5 are El Niño conditions. Therefore, we compare the two resulting SST sets to the climatological mean SST. In the case of SPEEDY, we conduct a ten year control run from January 1979 to December 1988. For this analysis, the climatological mean is the mean SST during this ten year time span of the months January to June. Similarly to the SPEEDY climatological mean, we obtain the climatological mean SST for ERA5 by calculating the average SST provided by ERA5 between 1979 and 1988. Again, we only consider the months January to June. The resulting anomalies are the difference between the mean SST from January to June 2016 and the respective climatological mean SST, and are illustrated in fig. 8. In both cases, the SST is higher during the months January to June 2016 than the average SST near the equator between 180°E and the west coast of South America, implying an El Niño event. SPEEDY includes the expected negative SST anomalies surrounding the warm region, as we can see in fig. 8. This indicates, that the data set providing SPEEDY with SST data induces practically ideal El Niño conditions. In the case of ERA5, the expected cold regions are not visible, apart from small regions around 40°N and 40°S . We must also note the difference in anomaly values. For SPEEDY, the anomalies reach a maximum of 1 K. The ERA5 anomalies, however, reach up to 2 K in the El Niño region. This means, that the El Niño event given in SPEEDY is not as strong as that in ERA5, which must be considered during the proceeding analysis.

Now that the existence of an El Niño event during January and June 2016 in both SPEEDY and ERA5 has been verified, we continue by comparing the two SST in order to determine where SPEEDY differs from ERA5. The comparison is visualized in fig. 9. Figures 9a) and b) show the mean SST of SPEEDY and ERA5, respectively. Overall, ERA5 seems to give higher SST values than SPEEDY. This we can verify by calculating the difference in SST between SPEEDY and ERA5, which is given in fig. 9e). However, as we can see, the difference in SST in the pacific ocean is mainly between -1 K and 1 K .

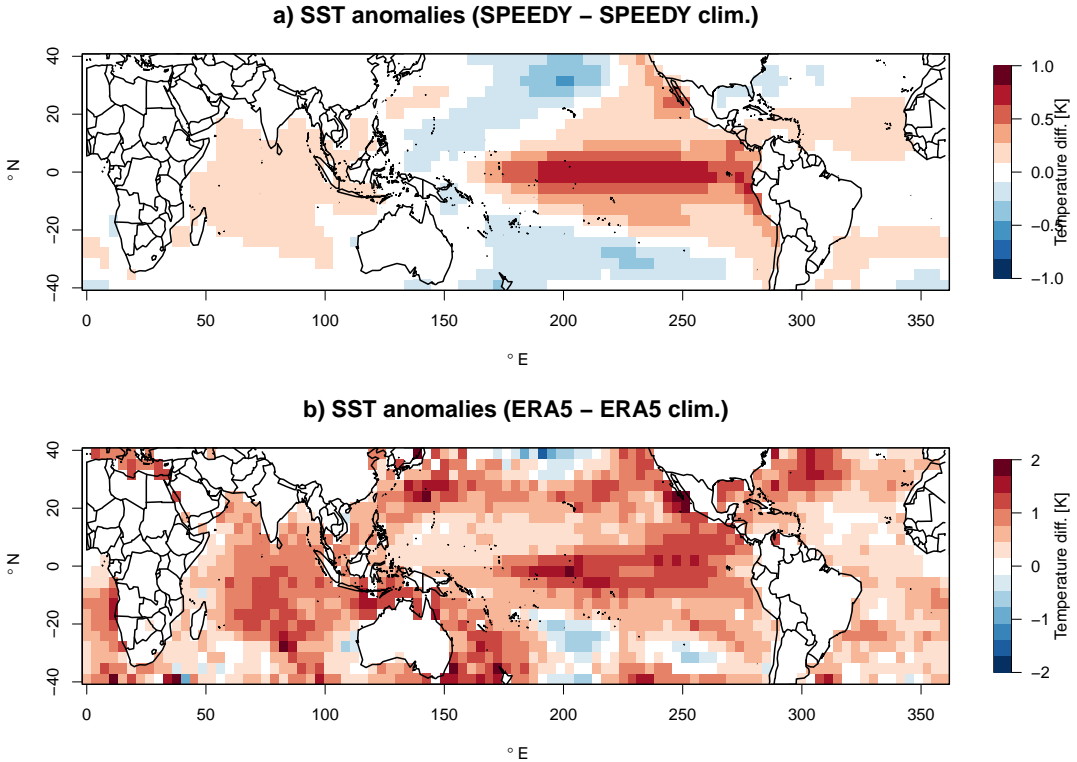


Figure 8: a) mean SST anomalies from January to June 2016 from SPEEDY compared to the mean SST from the control run. b) mean SST anomalies in the same time period from ERA5 compared to the climatological mean SST of ERA5.

In both cases, the SST in the pacific ocean practically doesn't vary, as is illustrated in figs. 9c) and d). Here, the standard deviations of the SST are illustrated. In the El Niño region, the SST remains almost constant, with variations reaching up to 1K for SPEEDY, and up to 2K for ERA5, however for only a small patch of ocean. Like for SPEEDY, the variation mainly lies between 0K and 1K. Within the El Niño region, the standard deviation of SPEEDY is lower than that of ERA5, as can be determined when regarding fig. 9f), where we visualized the difference in SST standard deviation between SPEEDY and ERA5. This means, that SPEEDY uses SST data with less variation in the El Niño region than ERA5 gives. This difference in SST and SST variation between SPEEDY and ERA5 is also illustrated in fig. 9h), where we see the course of the mean SST of both SPEEDY and ERA5 over time. In January (month 1), SPEEDY's mean SST is at 297K, which is approximately 1K lower than the mean SST of ERA5, laying at around 298K. This difference decreases over time. While SPEEDY's SST remains nearly constant, ERA5 gives a decrease in SST. Last but not least, we compare the two SST sets by calculating the correlation. As the temporal evolution of the SST is greatly influenced by the seasonal cycle, we first subtract the monthly average SST of each month from the respective months from January to June 2016, for both SPEEDY and ERA5. That way, the resulting correlation is between the SST anomalies induced by the El Niño event. The results are illustrated in fig. 9g). While there are regions with a positive correlation, meaning both SPEEDY and ERA5 give an increase (or decrease) in SST anomalies over time, there are also large regions with a negative correlation. This means, that either the anomaly increases in said region for SPEEDY and decreases for ERA5, or vice versa.

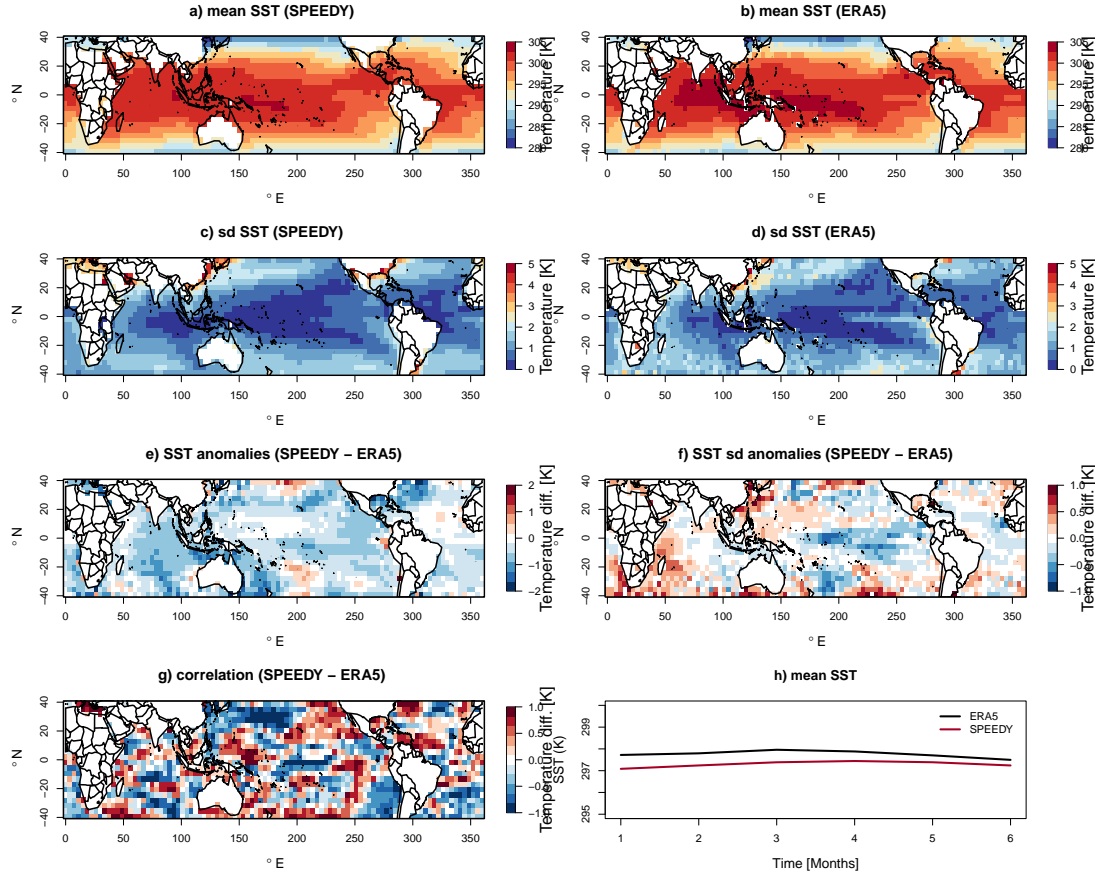


Figure 9: a) (SPEEDY) and b) (ERA5) mean SST, c) (SPEEDY) and d) (ERA5) SST standard deviation, e) difference in mean SST between SPEEDY and ERA5, f) difference in standard deviation between SPEEDY and ERA5, g) correlation between SPEEDY and ERA5 excluding the seasonal SST cycle, h) mean SST in the considered region over the six month period (month 1: January 2016, month 6: June 2016).

4.1.2 Precipitation

A comparison of the mean precipitation given by ERA5 from January to June 2016 with observational data (see fig. 10) shows, that ERA5 accurately reproduces the precipitation during the discussed time period, apart from a small region in the El Niño region and a couple outliers. In the El Niño region, anomalies lie mostly between $\pm 2 \text{ mm d}^{-1}$.

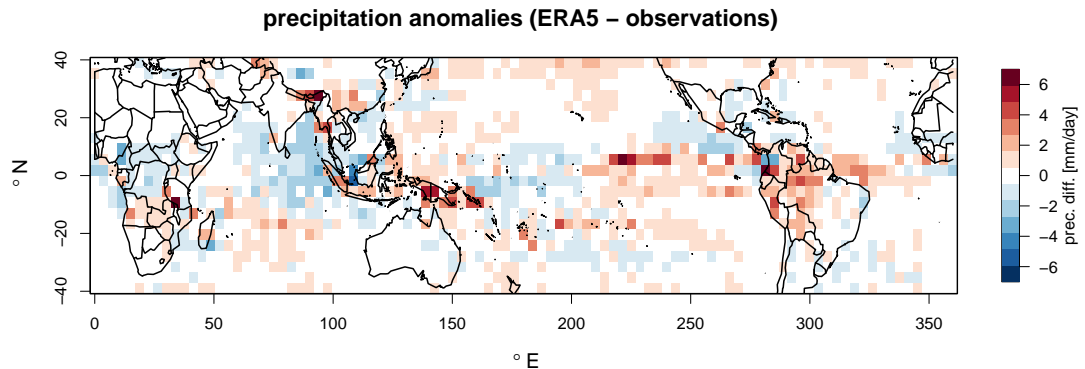


Figure 10: Mean precipitation anomalies of ERA5 compared to observational data.

Similarly to the sea surface temperature, we can compare the mean precipitation resulting from SPEEDY and ERA5 during January and June 2016 to the climatological average from January to June, in the years 1979 to 1988. The precipitation anomalies are illustrated in fig. 11, in fig. 11a) for SPEEDY and fig. 11b) for ERA5. In both plots we see an increased rain fall in the El Niño region, with a decreased precipitation in the surrounding areas. The amplitude of precipitation anomalies is lower for SPEEDY, reaching a maximum of 7.6 mm d^{-1} , than for ERA5. Here, we reach a maximum difference of 9.5 mm d^{-1} . This is consistent with the findings in section 4.1.1, where ERA5 gave a stronger El Niño event than SPEEDY, which can result in a larger precipitation anomaly compared to the climatological average precipitation.

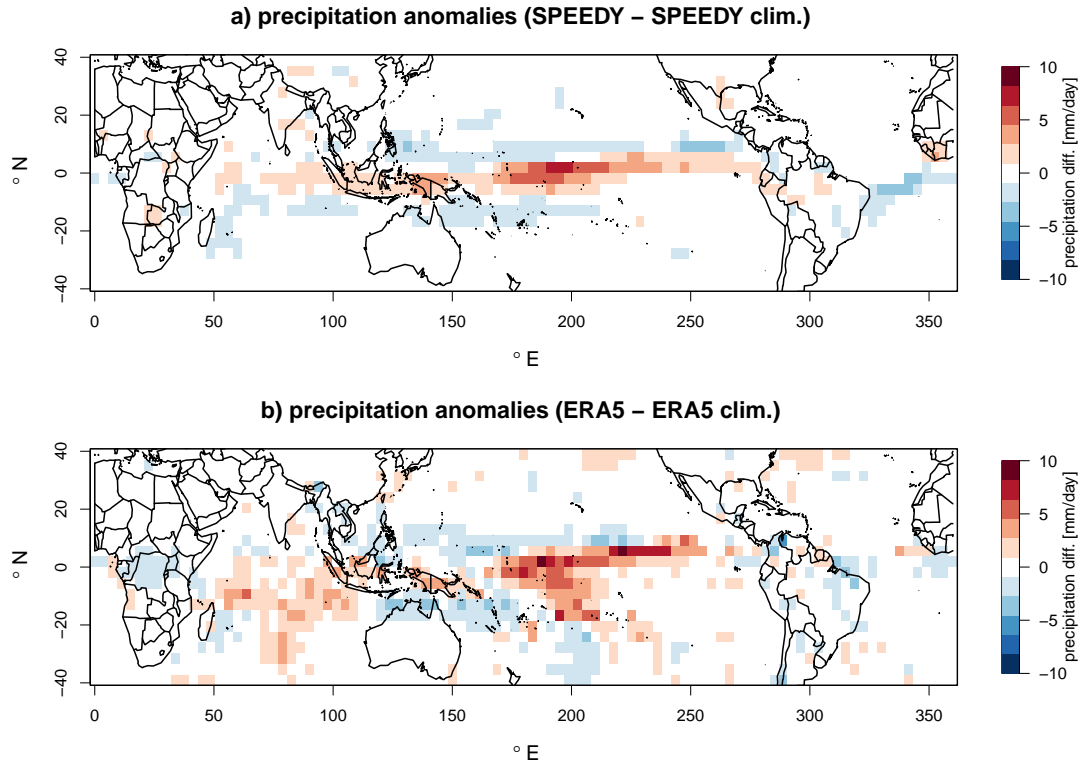


Figure 11: a) mean precipitation anomalies from January to June 2016 from SPEEDY compared to the mean precipitation from the control run. b) mean precipitation anomalies in the same time period from ERA5 compared to the climatological mean precipitation of ERA5.

However, when comparing the mean precipitation between January and June 2016 (shown in fig. 12a) and b)), we notice that SPEEDY's El Niño results in a higher mean precipitation. This does not coincide with the stronger El Niño event in ERA5 compared to SPEEDY. The difference in precipitation is visualized in fig. 12e). Along the equator in the pacific ocean and in the east of Brazil, the precipitation obtained using SPEEDY is up to 15 mm d^{-1} higher than that obtained from ERA5. Below or above said regions, the anomalies are negative, meaning SPEEDY gives lower precipitation rates than ERA5. However, in both cases the precipitation varies only slightly over time, as can be seen in fig. 12c) and d), and the difference in variation is very small in the El Niño region, apart from individual outliers. While the temporal evolution of the mean precipitation from both SPEEDY and ERA5, visualized in fig. 12h), are very similar to one another and only show negligible differences, the precipitation anomalies (mean precipitation excluding the climatological monthly average) show very little correlation, as shown in fig. 12e). Only between 150°E and 190°E , we see a region with predominantly positive correlation coefficients.

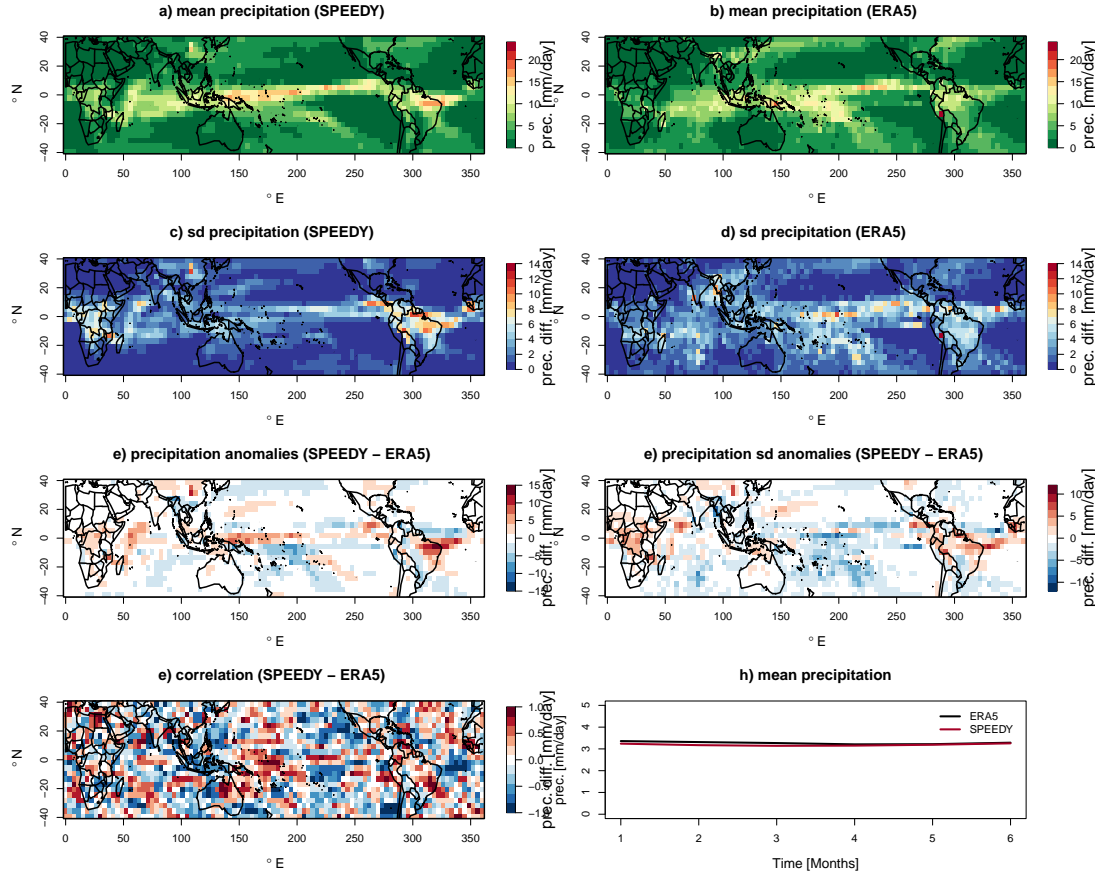


Figure 12: a) (SPEEDY) and b) (ERA5) mean precipitation, c) (SPEEDY) and d) (ERA5) precipitation standard deviation, e) difference in mean precipitation between SPEEDY and ERA5, f) difference in standard deviation between SPEEDY and ERA5, g) correlation between SPEEDY and ERA5 excluding the seasonal precipitation cycle, h) mean precipitation in the considered region over the six month period (month 1: January 2016, month 6: June 2016).

4.1.3 Wind and Circulation

As a comparison of the winds given by ERA5 with observational data is not possible in great detail, we are not able to verify the accuracy of the reanalyzed winds. Therefore, we include an additional reanalysis data set, namely NCEP, which we also compare to the winds given by SPEEDY. The mean winds from SPEEDY, ERA5, and NCEP are illustrated in figs. 13a), b), and c), respectively. In all three cases, the dominant wind direction in the El Niño region is westward, with a small component pointing south. The wind strength maximum in said region is at around 15 °N and on the west coast of South America. Near the equator, east of Indonesia, it is calm.

There are definite differences between the winds given by SPEEDY and those given by the reanalysis data sets, as we can see in fig. 14. Both figures, figs. 14a) and b), show, that SPEEDY's winds in the El Niño region, at $\pm 15^{\circ}\text{N}$, are weaker than for both reanalysis data sets. However, the winds given by SPEEDY are stronger near the equator in the El Niño region. This could be a reason as to why SPEEDY estimates higher precipitation in that region than ERA5. Weaker winds outside of the equator region can result in less moisture being transported into those areas. This can result in higher rainfall near the equator and lower rainfall farther North and South.

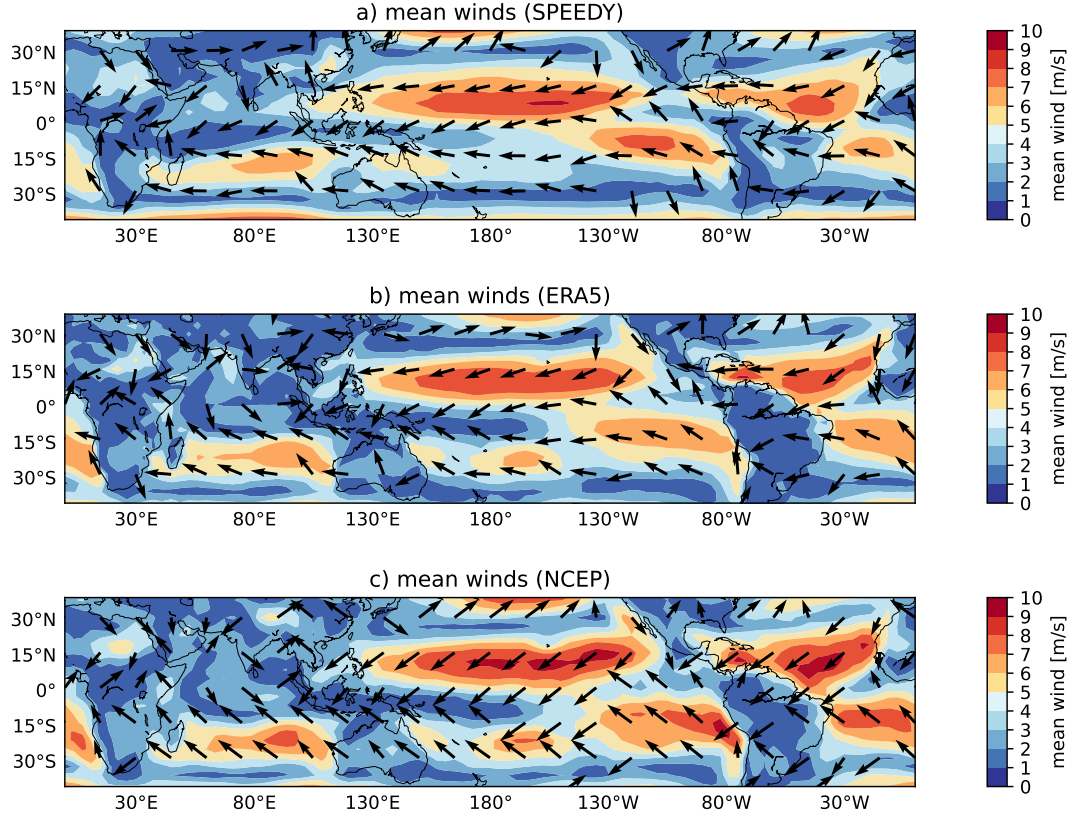


Figure 13: Mean winds from January to June 2016. Arrows represent the wind direction, the filled contour gives the wind strength. a) SPEEDY, b) ERA5, c) NCEP.

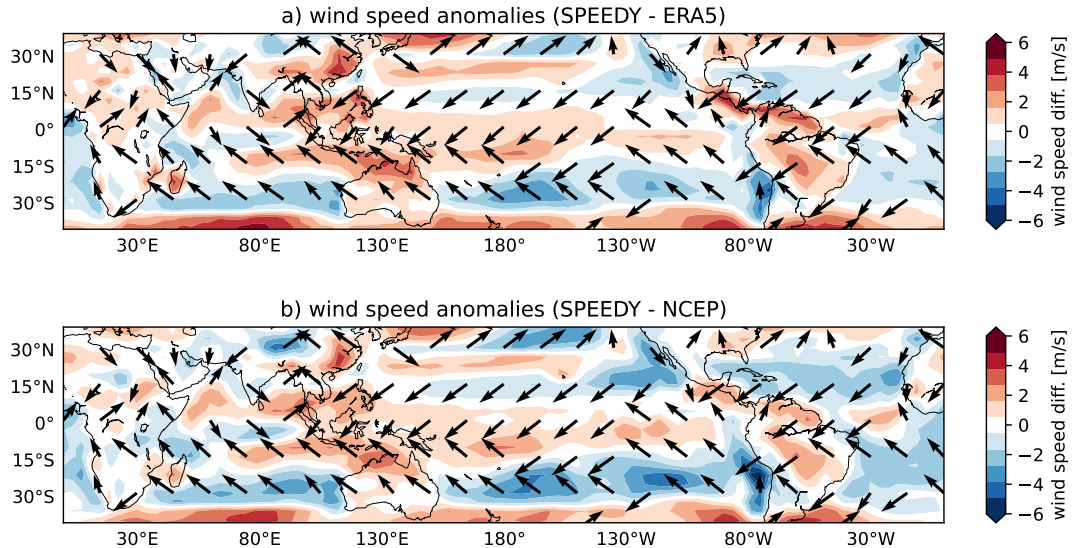


Figure 14: Wind speed anomalies in contour, a) SPEEDY compared to ERA5, b) SPEEDY compared to NCEP. The arrows represent the normalized wind vectors from SPEEDY.

4.2 La Niña

4.2.1 Sea surface temperature

The first parameter to investigate is the sea surface temperature. The first step is to investigate if the SPEEDY data set and the ERA5 data set each show La Niña conditions for the investigated time frame of July to December 2016. For this the ERA5 data of the six months time frame is compared to an observational data set for the six months time frame, which in contrast to the reanalysis data is not from the year 2016 but from 1979 to 1988, by plotting the anomalies. This is done to see if the reanalysis data is displaying La Niña conditions correctly compared to the typical conditions in this time frame of six months. The same comparison is done for SPEEDY with the exception that another SPEEDY model run from 1979 to 1988 was used instead of the observational data.

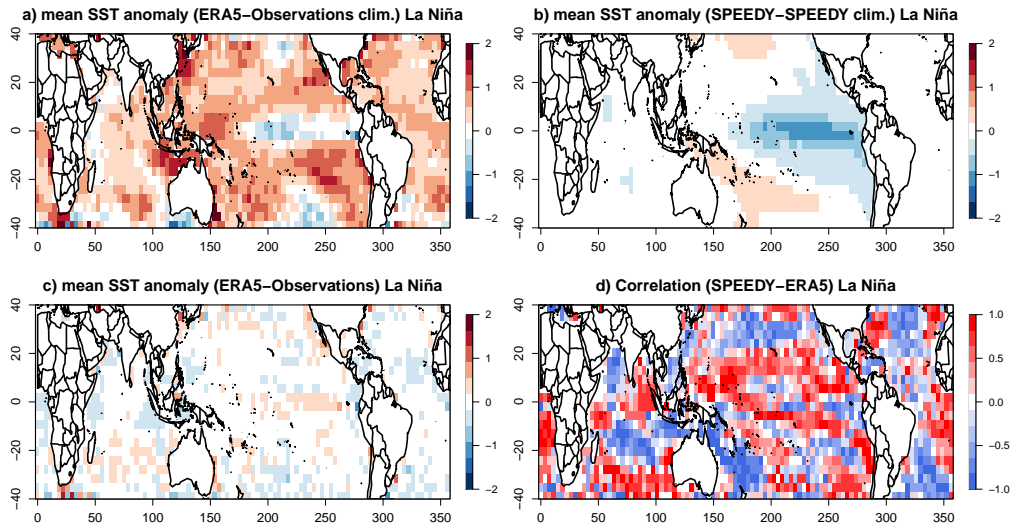


Figure 15: Mean Sea surface temperature anomalies. a) displays the anomaly between ERA5 (July-December 2016) and the long-term observations (July-December 1979-1988), b) shows the anomaly of SPEEDY (July-December 2016) and the SPEEDY control run (July-December 1979-1988) and c) displays the anomaly of ERA5 and the observations, both data sets of July to December 2016. Red indicates a positive anomaly where the ERA5/SPEEDY data for the event was higher than the compared data set and blue indicate a negative anomaly where the ERA5/SPEEDY data for the event was lower than the compared data set. The values are given as temperature with the unit of K. d) shows the correlation between SPEEDY and ERA5 for July to December 2016 without the seasonal cycle. A positive correlation (red) means the data sets move in the same direction and a negative correlation (blue) means the values move in opposite directions.

Figure 15a) displays the mean sea surface temperature anomaly of ERA5 (July - December 2016) and the long-term observations (July-December 1979-1988). The anomaly in the east Pacific by the northern part of south America is negative, indicated by the blue color, which means that the sea surface temperatures given by ERA5 are colder than the observed temperatures. This is the region where the temperatures are colder than normal at a La Niña event. Figure 15b) shows the mean sea surface temperature anomaly of SPEEDY (July - December 2016) and the SPEEDY control run (July-December 1979-1988). The figure displays the same area of cool sea surface temperatures in the Pacific which is bigger compared to the one in figure

15a). The anomaly is close to zero in almost every other area aside from the north at 40 °N and east of Australia, where the anomaly is positive indicating that the temperatures were higher than normal in 2016. These results fits the ideal La Niña conditions well.

Figure 15c) displays the anomaly of ERA5 and the observations, both data sets in the range from July to December 2016. This plot is used to control if the reanalysis data is showing good results compared to the observations for this specific time frame. The anomalies in this case are much smaller compared to the other two figures, as it lays between ± 0.5 K, which indicates that the ERA5 data agrees well with the observations for the sea surface temperature.

Figure 15d) shows the correlation of the SPEEDY data and the ERA5 reanalysis data without the seasonal cycle. The plot shows a mixture of positive correlation close to 1 and a negative correlation close to -1. There is a big area in the Pacific ocean that indicates a positive correlation, which means that the trend of both data sets is the same.

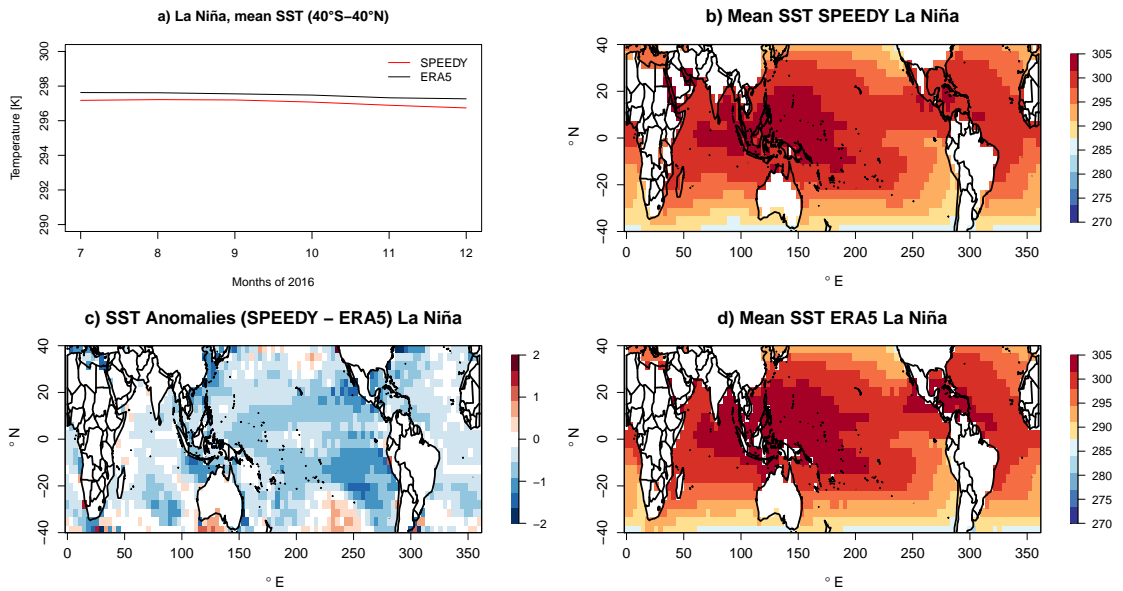


Figure 16: Mean Sea surface temperature comparison between SPEEDY and ERA5 for July-December 2016. a) displays a line plot for the mean sea surface temperature, averaged between 40 ° S and 40 ° N for all six months, b) shows the SPEEDY mean sea surface temperature (July-December 2016), c) displays the anomaly of SPEEDY and ERA5 and d) shows the ERA5 mean sea surface temperature. The values are given as temperature with the unit of K.

After the investigation if the SPEEDY and reanalysis data show La Niña conditions, which indeed they do, the two data sets are now compared to each other in figure 16. Figure 16a) suggests that the ERA5 reanalysis data is about 0.5 K higher than the SPEEDY data over the whole six months of the comparison. Figure 16b) and 16d) show the mean sea surface temperatures by SPEEDY and ERA5. It is noticeable that the average over all six months is also higher for ERA5 compared to SPEEDY. This is most noticeable in the area with the maximum temperatures around Indonesia. This observation can be validated with figure 16c) which shows the anomaly of both data sets. Aside from the areas around 40°N and 40°S the plot almost only shows blue areas with a few white areas in between. Especially in the Pacific ocean around the equator the figure shows the darkest blue areas, which means that the SPEEDY data

in these areas is smaller than the ERA5 reanalysis data. The differences of the temperatures are highest with a value of around 1 K.

4.2.2 Precipitation

The second parameter to investigate is the precipitation. Again, the first step is to investigate if the SPEEDY dataset and the ERA5 dataset each show La Niña conditions for the time frame of the comparison from July to December 2016. This is done in the same way that it was done for the sea surface temperature.

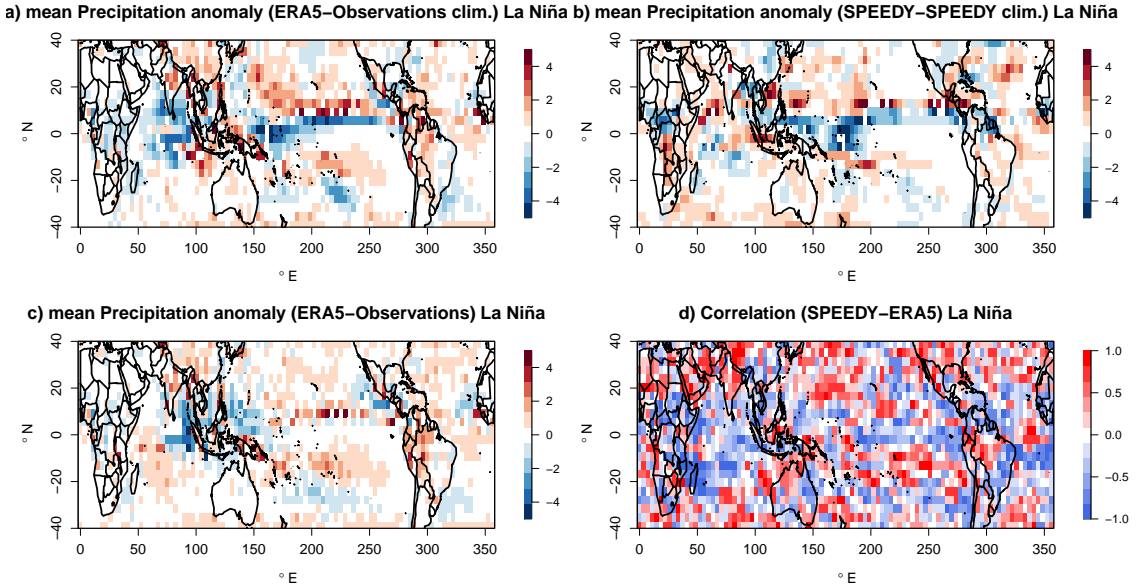


Figure 17: Mean precipitation anomalies. a) displays the anomaly between ERA5 (July-December 2016) and the long-term observations (July-December 1979-1988), b) shows the anomaly of SPEEDY (July-December 2016) and the SPEEDY control run (July-December 1979-1988) and c) displays the anomaly of ERA5 and the observations, both data sets of July to December 2016. Red indicates a positive anomaly where the ERA5/SPEEDY data for the event was higher than the compared data set and blue indicate a negative anomaly where the ERA5/SPEEDY data for the event was lower than the compared data set. The values are given in mm/day. d) shows the correlation between SPEEDY and ERA5 for July to December 2016 without the seasonal cycle. A positive correlation (red) means the data sets move in the same direction and a negative correlation (blue) means the values move in opposite directions.

Figure 17a) displays the mean precipitation anomaly of ERA5 (July-December 2016) and the long-term observations (July-December 1979-1988). The anomaly in the Pacific around the equator between Indonesia and middle America is negative, indicated by the blue color, which means that the precipitation given by ERA5 are less compared to the normal state given by the observational data. Compared to figure 3 this is similar to the ideal La Niña conditions regarding the precipitation.

Figure 17b) shows the mean sea surface temperature anomaly of SPEEDY (July-December 2016) and the SPEEDY control run (July-December 1979-1988). The figure shows the same

area of low precipitation in the Pacific as figure 17a). The anomaly at around 10°N and 10°S is positive in both plots, meaning that there was more precipitation than normal. These results fits the ideal La Niña conditions well.

Figure 17c) displays the anomaly of ERA5 and the observations, both data sets of July to December 2016. This plot is used to control if the reanalysis data is showing good results compared to the observations for this specific time frame. The anomalies in this case are a little smaller compared to the other two figures in the Pacific ocean. Aside from the area directly north of Australia the anomaly at the equator in the Pacific is close to zero, which suggests that the ERA5 data is in agreement with the observations in the La Niña area.

Figure 17d) shows the correlation of the SPEEDY data and the ERA5 reanalysis data without the seasonal cycle. The plot shows a mixture of positive correlation close to 1 and a negative correlation close to -1. The correlation in the Pacific around the equator is negative in the most parts which means that the trend in the data sets are opposite. As the plot shows a mixture of positive and negative correlation it is not easy to interpret.

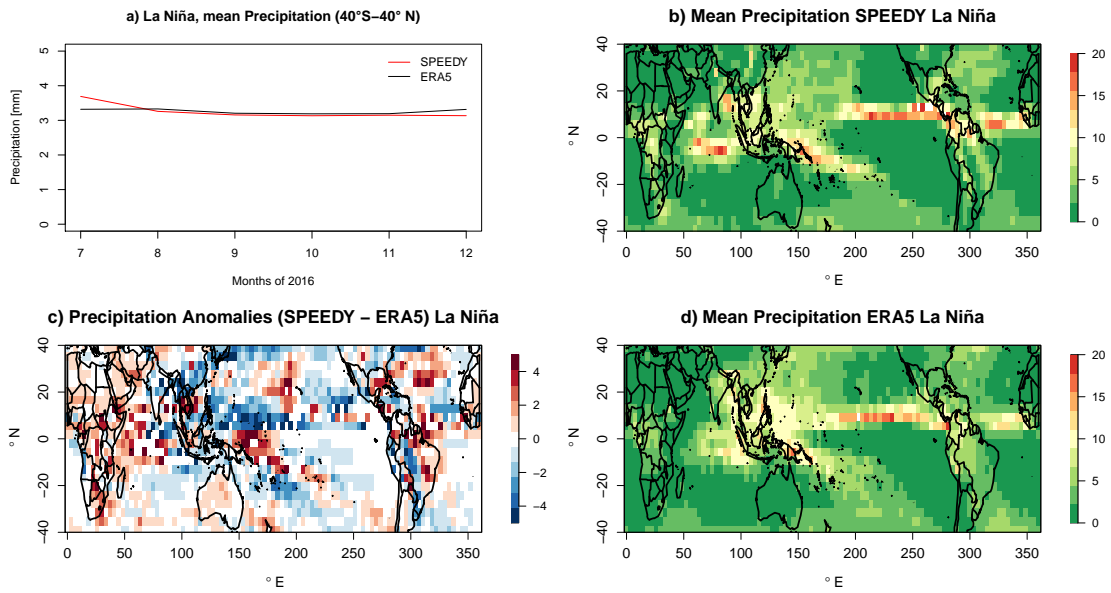


Figure 18: Mean precipitation comparison between SPEEDY and ERA5 for July-December 2016. a) displays a line plot for the mean precipitation, averaged between 40°S and 40°N for all six months, b) shows the SPEEDY mean precipitation (July-December 2016), c) displays the anomaly of SPEEDY and ERA5 and d) shows the ERA5 mean precipitation. The values are given in mm/day.

After the investigation if the SPEEDY and reanalysis data show La Niña conditions, which in this case they also do, the two data sets are now compared to each other in figure 18. Figure 18a) suggests that the SPEEDY data is about 0.5 K higher than the ERA5 reanalysis in the month of July 2016. From August onward the SPEEDY data is lower but very close to the data values of the reanalysis, only in the month of December 2016 there is a more noticeable difference of about 1 mm/day again. Figure 18b) and 18d) show the mean precipitation by SPEEDY and ERA5. It is noticeable that the average over all six months shows a similar pattern for SPEEDY and ERA5 with the maximum in the Pacific Ocean at 10°N and a minimum in the Pacific at the equator. Figure 18c) shows that the data sets agree well at the equator in the Pacific with

the exception of the west Pacific. SPEEDY gives a higher precipitation north of Australia than ERA5, but a lower precipitation at 10 °N between Indonesia and middle America. The differences of the precipitation are between ± 4 mm/day in these areas.

4.2.3 Wind and Circulation

The last parameter to investigate is the wind. In this case a second reanalysis data set, NCEP, is used to investigate the correctness of the ERA5 data. Figure 19 shows the mean wind speeds and directions for all three data sets.

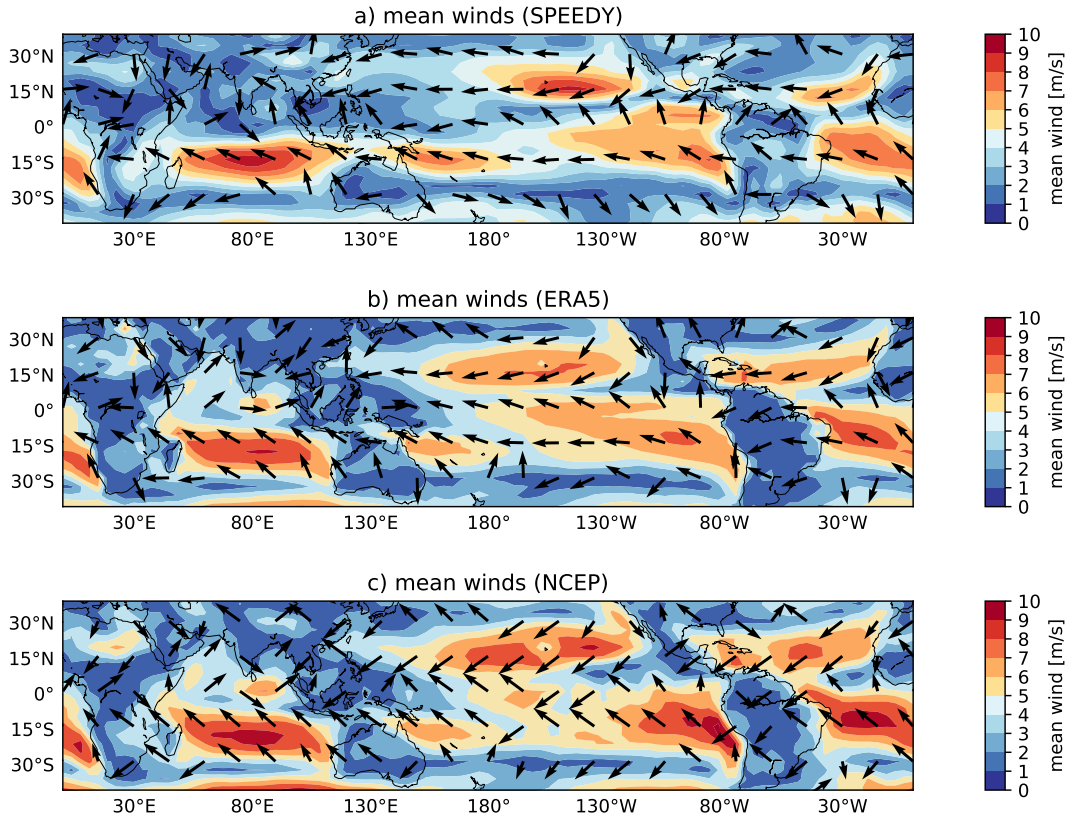


Figure 19: Mean winds comparison between SPEEDY, ERA5 and NCEP for July-December 2016. Displayed are the mean wind speeds and directions : a) obtained from SPEEDY, b) given by ERA5 and c) obtained from NCEP. The values are given in m/s.

The areas with the highest wind speeds are roughly the same in all three plots, although they vary in size and values. The highest wind speeds are seen over the Oceans. The NCEP data shows the highest values of about 10 m/s in the east Pacific. Recalling figure 4 there should be east winds in the Pacific around the equator. This can be seen in both figure 19a) and 19b). Figure 19c) shows southeast winds in the same areas, which means there are differences between the reanalysis data sets. Regarding the wind directions ERA5 seems to be able to show the SPEEDY and therefore La Niña conditions better than the NCEP reanalysis data, but it is difficult to make a statement about that by only investigating two reanalysis data sets.

4.3 IOD+

4.3.1 Sea surface temperature

The first parameter being investigated is the sea surface temperature.

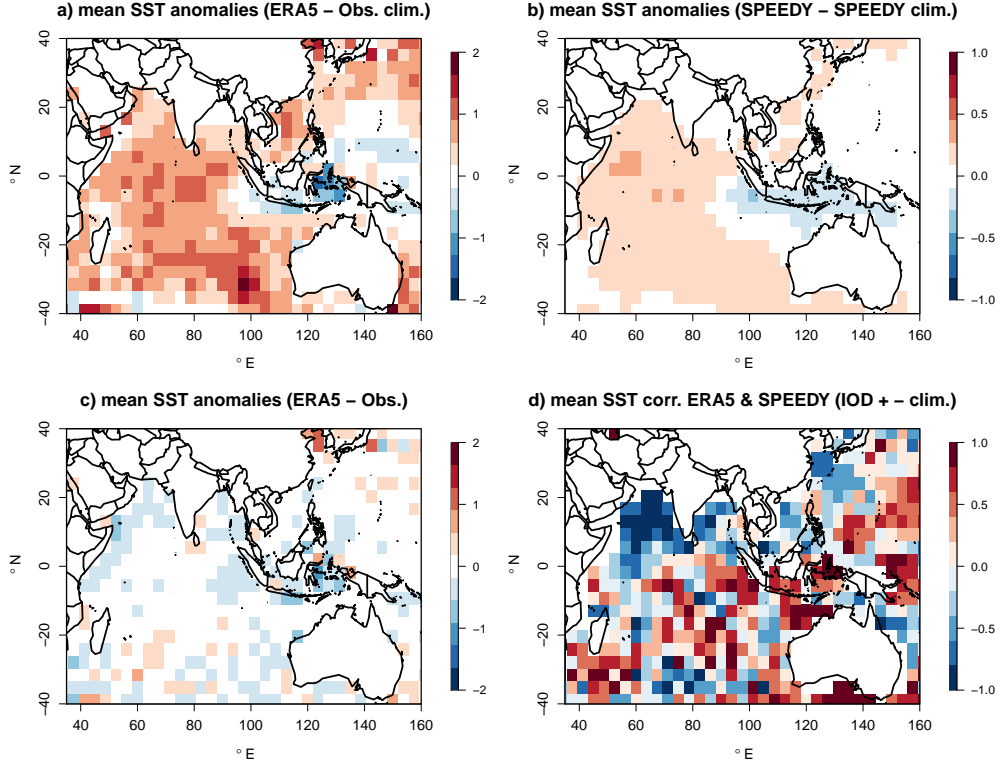


Figure 20: Sea Surface Temperature anomaly contour plots (in K). a) ERA5 reanalysis (IOD+ event) - Observations (10 year climate state); b) SPEEDY (IOD+ event) - SPEEDY (10 year climate state); c) ERA5 reanalysis (IOD+ event) - Observations (IOD+ event); d) Correlation between ERA5 and SPEEDY without the seasonal cycle (scale has no unit).

In figure 20a) (b)), the anomalies between the ERA5 reanalysis data (the SPEEDY model output) for the time period of the IOD+ event and the climate state of the observations (climate state of SPEEDY) are visualized. Both plots should therefore show a SST distribution similar to the idealized graphic with colder water around Indonesia and Australia and warmer water in the western Indian Ocean. This distribution can be seen in the plots, but the region of warmer SST extends further eastwards for both ERA5 and SPEEDY. Additionally, the anomalies between SPEEDY and its climate state are in general much smaller than between ERA5 and the long time observed climate data.

In figure 20c) the anomalies between the ERA5 data and the observations, now both for the six month period of the event, are shown. The anomalies are mostly below 0.55 K in any direction, while in most areas ERA5's SSTs are slightly lower than those measured. All in all, ERA5 seems to stray not too far away from the observations.

Plot 20d) shows the correlation between the ERA5 and the SPEEDY SST data for which the seasonal cycle has been removed. As for the El Niño and La Niña event, a mixture of strong positive and negative correlations can be observed, with sudden changes of regimes on a regional scale. However, there is a patch of strong negative correlation in the northwest Indian Ocean

indicating a divergence of the data sets in this area of warmer temperatures during the IOD+ event. Also the correlation is mostly close to 1 in the Indonesian region, which hints towards a good agreement between both data sets in this region.

Since both ERA5 and SPEEDY are capable of recreating the coarse pattern of SST distribution during an IOD+ event and the anomalies between ERA5 and the observations are rather small during this event, ERA5 is useful for an assessment of SPEEDY's ability to forecast the SST. This will be done using the following plots.

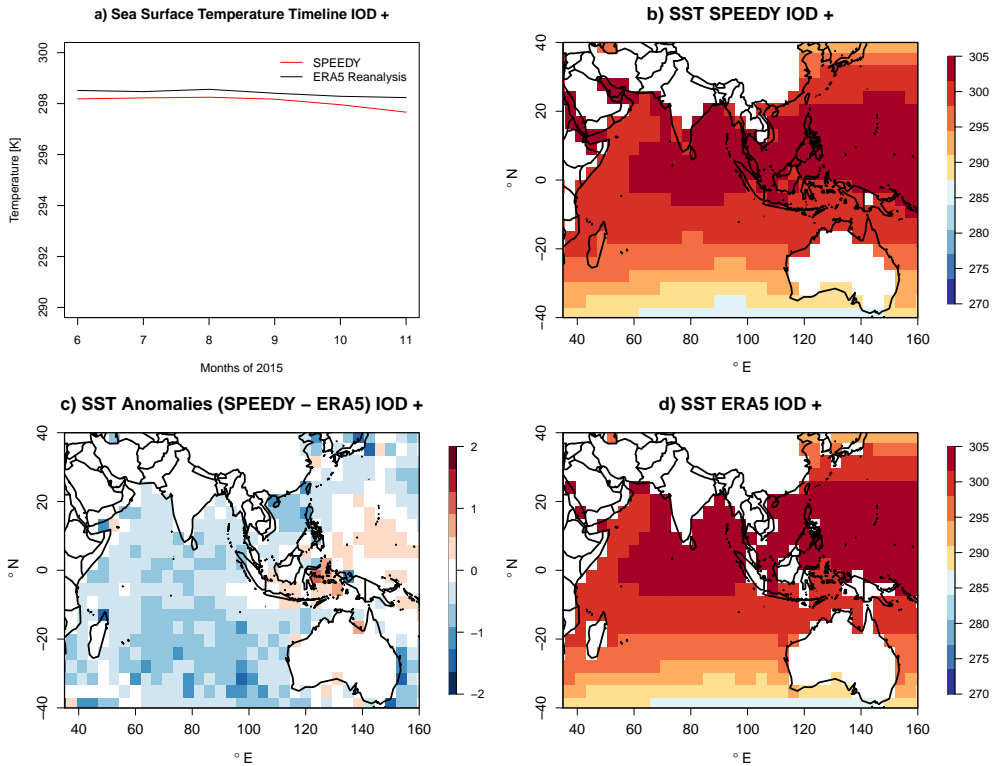


Figure 21: Sea Surface Temperature plots for IOD+ event (in K). a) Line plot for time evolution of SPEEDY and ERA5 reanalysis data; b) SPEEDY; c) Anomalies SPEEDY - ERA5 ; d) ERA5 reanalysis.

The figure 21a) shows the development of the SST given by SPEEDY and ERA5 for the Indian Ocean region. With both average temperature curves laying around 298 K, SPEEDY always yields slightly lower temperatures with the anomaly increasing towards the end of the year. In the plots 21b) and d) the sea surface temperature given by SPEEDY and the ERA5 reanalysis are visualized respectively. While the qualitative distribution of the SST appears to be quite similar in both plots, one can see that for SPEEDY the colder water extends a little bit further to the north between 80° and 100° E, which might lead to negative anomalies between SPEEDY and ERA5. Plot 21a) suggests that this process might have an increased influence in late autumn. Closer investigation of figure 21c) confirms this. SPEEDY yields colder temperatures for most of the Indian Ocean apart from the region around Indonesia, where the SST given by SPEEDY is warmer. Comparing these observations with the idealized case in figure 5, SPEEDY seems to underestimate the temperature in the regions of warmer SST and to overestimate the SST in the regions of colder temperature during IOD+. Similar to the the plots 20a) and b), where the regions of warmer SST are both extended further eastwards than in the idealized case, the region of negative anomalies are present throughout the whole Indian Ocean in the

plot 21c). This supports the suspicion, that SPEEDY underestimates the warm SST anomalies of the IOD+ event in comparison to the climate measurement standard and overestimates the SST in the regions of colder SST during the event.

4.3.2 Precipitation

The second climatological variable being part of this assessment is the precipitation.

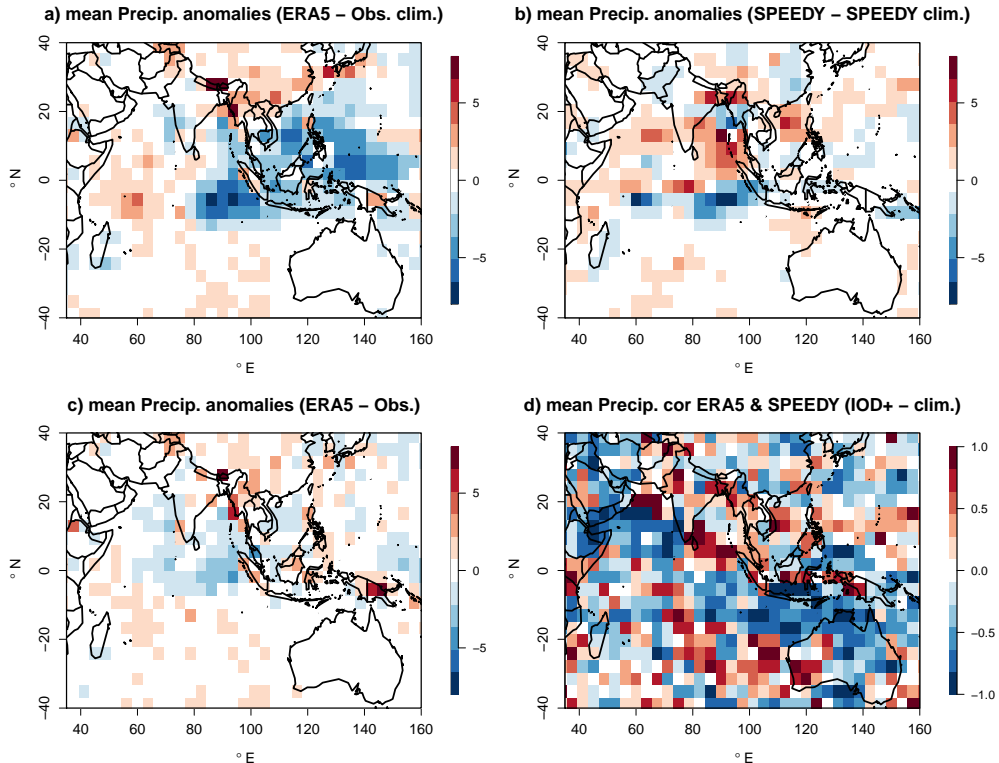


Figure 22: Precipitation anomaly contour plots (in mm/day). a) ERA5 reanalysis (IOD+ event) - Observations (10 year climate state); b) SPEEDY (IOD+ event) - SPEEDY (10 year climate state); c) ERA5 reanalysis (IOD+ event) - Observations (IOD+ event); d) Correlation between ERA5 and SPEEDY without the seasonal cycle (scale has no unit).

Figures 22a) and b) visualize the anomalies between the ERA5 reanalysis data respectively the SPEEDY model output for the time period of the IOD+ event and the climate state of the observations respectively the climate state of SPEEDY. Both graphics should show enhanced precipitation over the Horn of Africa and lessened precipitation around Indonesia and Australia. While the ERA5 data (figure 22a)) manages to show a declining precipitation around Indonesia, there seems to be no significant increase over East Africa. For SPEEDY, the area of lessened precipitation during the IOD+ event in the east is less prominent and moved a bit southwestwards while again there is no significant increase of precipitation over the Horn of Africa. In figure 22c) the anomalies between the ERA5 data and the observations, now both for the six month period of the event, are shown. The anomalies are mostly below 2 mm/day in any direction. The figure suggests that ERA5 predicts slightly too dry zones where the rainfall is supposed to decrease during IOD+. Also there are no big anomalies over East Africa, suggesting that while both ERA5 and SPEEDY fail to show higher precipitation in this region,

this might not be a model error since the observations are also not showing enhanced rainfall for this particular IOD+ event i.e. there are no significant anomalies between ERA5 and the observations in the time frame of the event.

Lastly, the plot 22d) visualizes the correlation between the precipitation data given by ERA5 and SPEEDY, again without including the seasonal cycle. Once more, a seemingly random mixture of strong positive and negative correlations changing on a regional scale can be observed. Most notably, there is one large patch of mediocre to strong negative correlation between Indonesia and the south coast of Australia. In this region, the ERA5 and SPEEDY output seem to develop differently over the course of the evaluated time frame.

Since ERA5 is again capable of recreating the coarse pattern of precipitation distribution during the IOD+ event and the anomalies between ERA5 and the observations are rather small, ERA5 can be used to assess SPEEDY's ability to forecast the precipitation. For that the following graphics are used

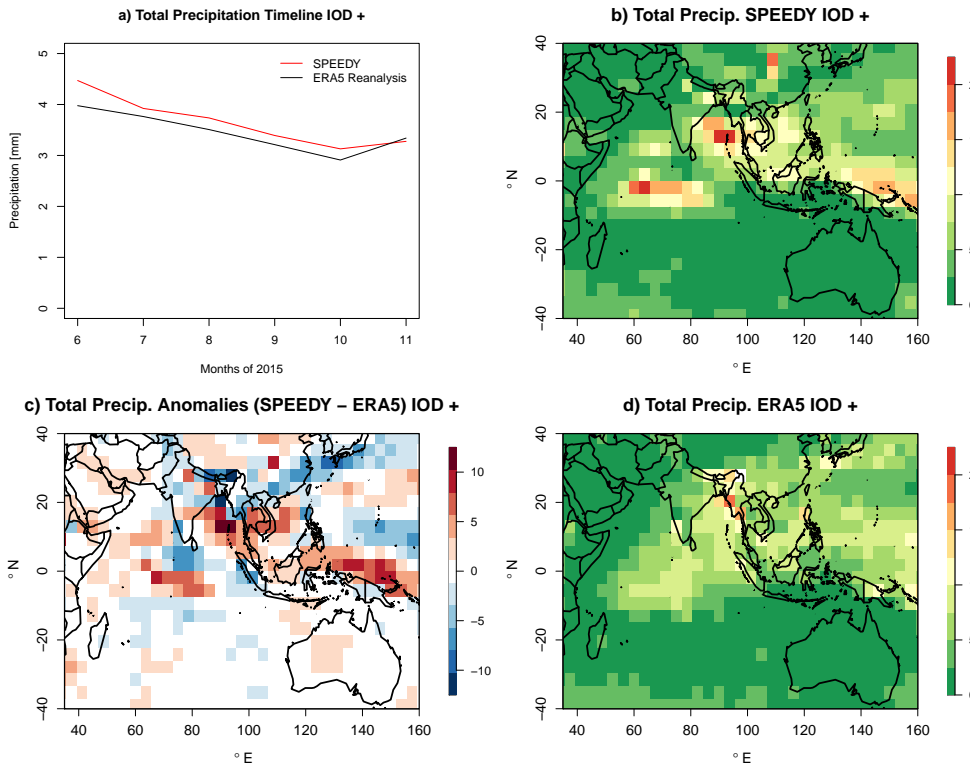


Figure 23: Precipitation plots for IOD+ event (in mm/day). a) Line plot for time evolution of SPEEDY and ERA5 reanalysis data; b) SPEEDY; c) Anomalies SPEEDY - ERA5 ; d) ERA5 reanalysis.

Again, figure 23a) shows the time development of the monthly averages given by SPEEDY and ERA5 for the Indian Ocean region, this time for the precipitation. Apart from November, SPEEDY yields slightly higher precipitation by about 0.2 mm/day in average compared to the ERA5 reanalysis data with the anomalies being biggest in June. In the plots 23b) and d) the precipitation from the SPEEDY output and the ERA5 reanalysis data are visualized respectively. For both plots, the areas of mediocre and high precipitation values (over 5 mm/day) are the same nearby and north of the equator starting from 60° E eastwards. But SPEEDY is calculating higher maximal values of precipitation, most notably in a patch around the equator in the Western Indian Ocean and east of India. This adds to the impression that the ERA5

precipitation is more uniformly distributed while for SPEEDY there are big differences in the precipitation on a regional scale in multiple places. This is backed up by the anomaly plot for the difference between SPEEDY and ERA5 during the IOD+ event in figure 23c). In the regions of stronger precipitation defined above, the anomalies are quite big with sometimes over 10 mm/day, while also the direction of anomalies (over-/underestimation of precipitation by SPEEDY compared to ERA5) varies regionally. Both effects are predominantly occurring between the equator and about 20° N.

4.3.3 Wind and Circulation

Lastly, the near-surface atmospheric circulation is compared for SPEEDY and two reanalysis data sets, whose data are visualized below.

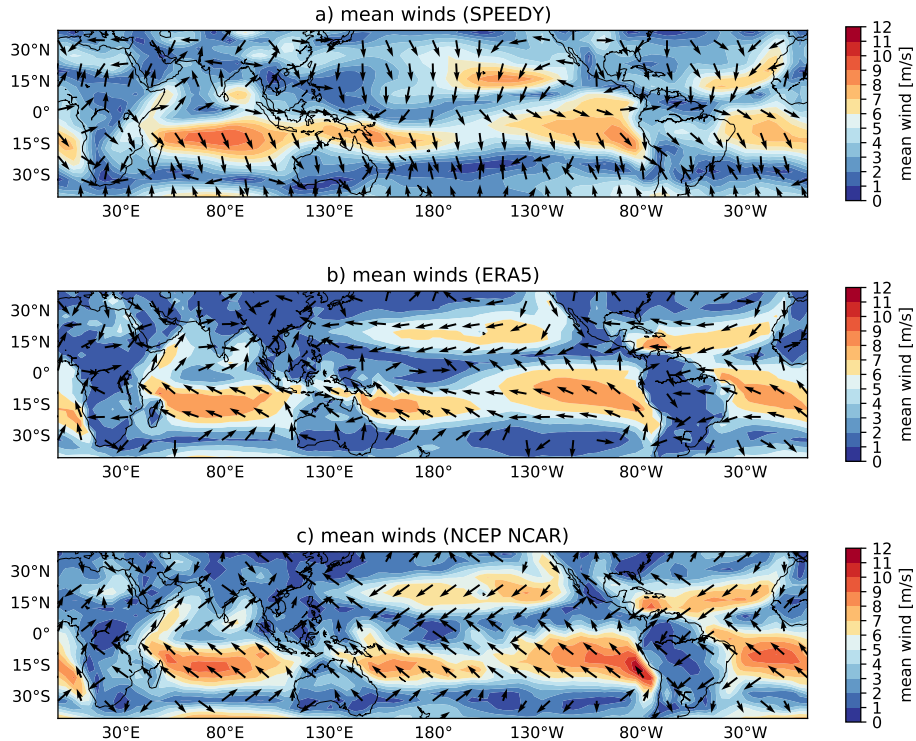


Figure 24: Wind Speed contour and arrow plots for IOD+ event. a) SPEEDY; b) ERA5 Reanalysis; c) NCEP NCAR Reanalysis.

The figures 24b) and c) show the tropic circulation system of the ERA5 and the NCEP NCAR reanalysis sets respectively. Both show a similar circulation scheme. While there are south west and west winds with an average speed of 2 to 6 m/s in the northern Indian ocean, the wind turns into a southeasterly direction south of the equator and the wind speed is considerably higher. While in this region, ERA5 forecasts wind speeds with an average between 5 and 8 m/s, NCEP NCAR yields average wind speeds of up to 10 m/s. Analyzing plot 24 a), one can see that the SPEEDY data gives a wind speed distribution comparable to the NCEP NCAR data with the area of increased wind speed laying a little more in the north for the climate model data. Alas, the wind direction given by SPEEDY in the Indian Ocean south of the equator is pointing southwards, so instead of southeasterly winds SPEEDY calculates northwest and north winds. Plus, SPEEDY's output shows south winds over India, hinting towards a big influence of the summer monsoon.

To gain more insight into the possible reasons for the SPEEDY model's difference in wind

directions compared to both reanalysis data sets, the SPEEDY circulation plots are split into the single months of the IOD+ event in the following graphic 25.

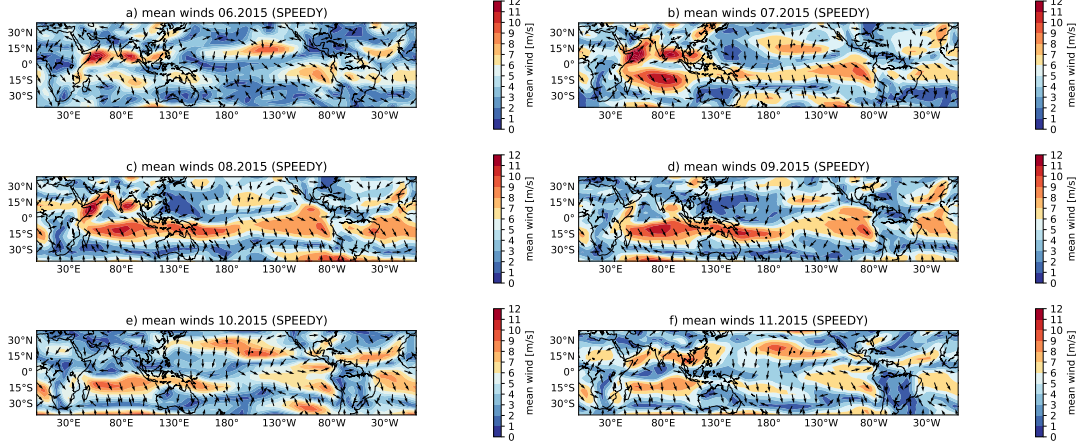


Figure 25: Wind Speed contour and arrow plots for IOD+ event (SPEEDY data only). The data is split up by the months (June to November 2015) of the IOD+ event.

Figure 25 shows the SPEEDY meridional and zonal wind output split up into the months from June to November 2015. These plots show two interesting aspects. Firstly, in the Indian Ocean north of the equator, it seems like the wind speed and direction is dominated by the summer and winter monsoon rather than by the IOD+ event. From June to August (figures 25a-c)), which is the time of the summer monsoon, there are strong southerly wind components heading northwards. In November (figure 25f)), where the winter monsoon starts to set in, the wind has turned into a northerly direction. The only month showing the expected direction of the wind nearby the equator for an IOD+ event is October (figure 25e)). Secondly, there is a southerly wind observed for every month in the Indian ocean south of the equator with the alteration only laying in the wind speed. While during July to September average wind speeds of up to 11 m/s are reached, June yields a more moderate wind with up to 8 m/s in that region. But in a whole, these results lead to the patch of fast northerly wind in the south-equator Pacific observed in the figure 24a) which is, at least in terms of the wind speed, backed up by both reanalysis sets.

4.4 IOD-

4.4.1 Sea Surface Temperature

In this part, the anomaly performance of SPEEDY versus reanalysis and observational data is evaluated. Sea surface temperature or ocean surface temperature is the water temperature. Firstly, analyzing the data sets helps to interpret SPEEDY's efficiency. It is clear that there are no large differences among the data sets. For instance, sub-figure 'a' shows maximal anomalies of 2 K. As can be seen by the scales of the figures, the intensity of the anomaly values are lower by 2-3 K. However, the anomalies are generally seen over the locations whose land and ocean are coupled, such as Indonesia.

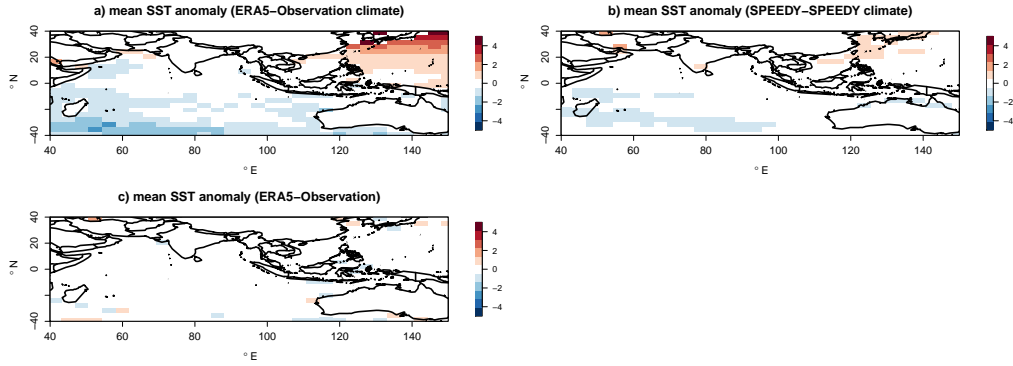


Figure 26: Mean SST anomalies among three different data. a) belongs to the anomalies between reanalysis and observational climate data, b) includes the anomalies of SPEEDY – SPEEDY climate data and c) has the anomalies between reanalysis and observational data.

In this figure, the SPEEDY output is compared to ERA5 data. In SPEEDY, the field of warmer temperature is wider than ERA5's. This difference can especially be seen in the eastern sides of Indonesia. In the anomaly plot, it is seen that the southern parts of the Indian ocean are warmer in ERA5. Oppositely, the northern sides of Indonesia is warmer according to SPEEDY. The cooler area by SPEEDY is larger than the warmer area given by the model. Though there are anomalies between Speedy and ERA5, they are not bigger than 4 K.

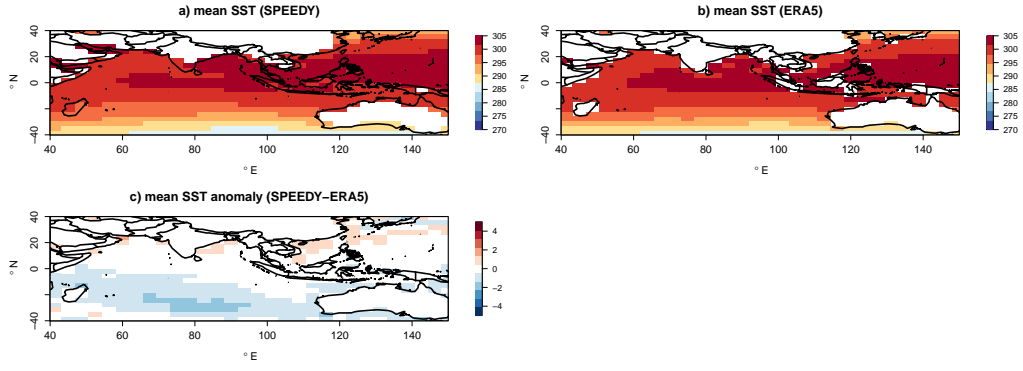


Figure 27: Mean SST of SPEEDY and reanalysis data. a) mean sea surface temperature of SPEEDY and b) mean sea surface temperature of reanalysis data (ERA). c) represents the anomaly between SPEEDY and reanalysis data.

4.4.2 Precipitation

The precipitation is one of the most challenging meteorological variables for both SPEEDY and reanalysis data sets, as it is easily affected by various types of variables such as temperature, relative humidity, and wind. Compared to the SST anomaly graphics, the precipitation anomalies are more complex so negative and positive anomalies are more pronounced. Among the different precipitation data sets, the lowest anomalies can be seen in the graphic between reanalysis data and observational data. Especially the regions where mostly convective movements happen have more differences in terms of the precipitation amount. These regions are mountain areas and land-ocean mixed geographical areas.

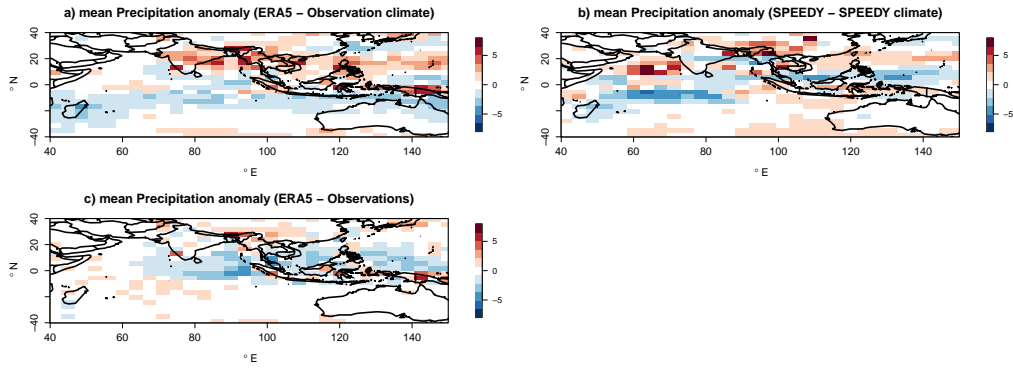


Figure 28: Mean precipitation anomalies of data sets. a) belongs to the anomalies between reanalysis and observational climate data, b) includes the anomalies of SPEEDY – SPEEDY climate data and c) has the anomalies between reanalysis and observational data.

As can be seen from the figures, SPEEDY shows more intense precipitation over the southern part of and east of the Indian peninsula. The anomaly plot in the sub-figure c supports this idea. Additionally, SPEEDY displays less intense precipitation over Indonesia. This anomaly behavior might be due to Indonesia being a mountain location with more convective motions.

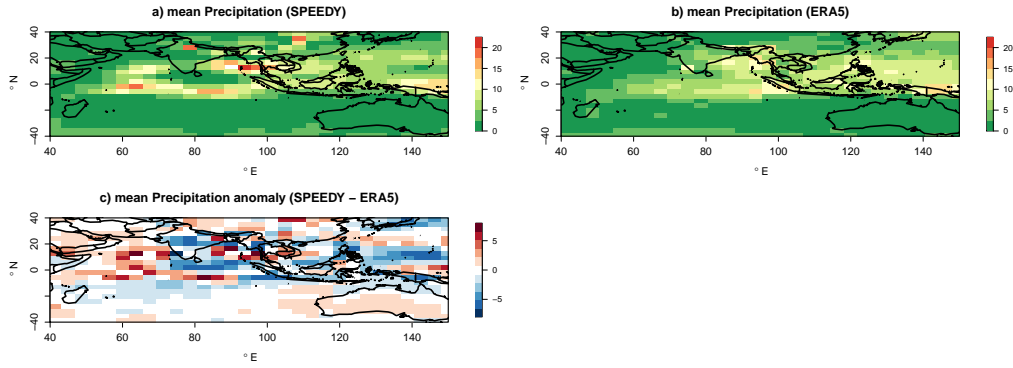


Figure 29: Mean precipitation of SPEEDY and reanalysis data. a) mean precipitation for SPEEDY and b) mean precipitation for reanalysis data (ERA). c) represents the anomaly between SPEEDY and reanalysis data.

4.4.3 Wind Circulation

In the wind part, the mean direction and intensity of both zonal and meridional winds are considered. Zonal wind direction is East-West, meridional flows also North-South direction in the hemisphere. In this part, we have no observational data, but have comparison among SPEEDY, reanalysis data (ERA5 and NCEP). The both mean wind speeds and its directions for all data sets are shown in Figure 30. The regions whose high wind speeds are generally in the same locations. However, their geographical size and intensities could be variable. Wind speeds that flow over the oceans have more strength than winds over the lands. Especially, the wind over Indian Ocean is stronger in the sub-figure c. SPEEDY has to be developed in order to catch directions of the winds because in sub-figure a and b in order, wind directions are generally meridional and zonal over Indian and Pacific ocean. Therefore, the differences between reanalysis data sets can be easily shown. In sub-figure c, patterns of trade winds are more accurate. In terms of effective regions and strength of the wind, SPEEDY performs optimal approaches. Because the regions where the wind is effective or not effective are not well-separated in SPEEDY.

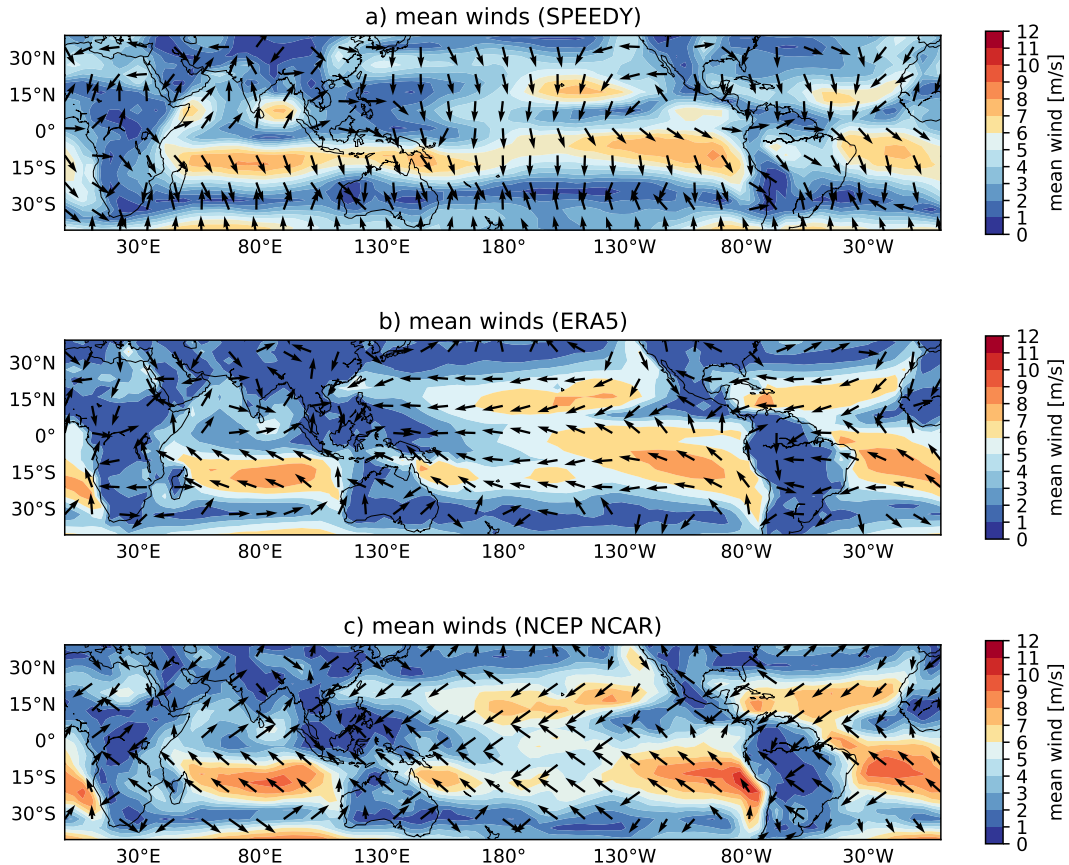


Figure 30: Mean wind speed and direction for the data sets.

5 Conclusion and outlook

In the case of the ENSO cycle, SPEEDY is able to reproduce the key features, such as the expected precipitation anomalies and regional circulation. However, a more detailed analysis of the results shows, that SPEEDY struggles with simulating the exact precipitation rates and wind speeds.

SPEEDY struggles more with recreating the IOD cycle. While the model is able to estimate the precipitation with only small anomalies, the wind directions simulated by SPEEDY differ significantly from those given by ERA5 and NCEP.

In this report, the focus was on the sea surface temperature, the precipitation, and the winds and circulation in the regions of ENSO and IOD. It would be interesting to extend the region, e.g. including North America, and all of Asia, as these continents are effected by ENSO and IOD. Furthermore, a similar analysis of other climate variables, such as relative humidity, surface pressure, or cloud coverage, can give more incite, as to how well SPEEDY is able to reproduce El Niño , La Niña, IOD+, and IOD-. Additionally, it is necessary to determine why SPEEDY's simulated circulation during the IOD events differs significantly from those given by ERA5 and NCEP.

References

- Copernicus. ERA5 monthly averaged data on single levels from 1979 to present: Download data. Webpage. 18.04.2019. <https://cds.climate.copernicus.eu/cdsapp#!/dataset/reanalysis-era5-single-levels-monthly-means?tab=form>. [Online: 17.02.2022, 13:34 PM]
- Dogar, M. M., F. Kucharski, T. Sato, S. Mehmood, S. Ali, Z. Gong, D. Das, J. Ar- raut. Towards understanding the global and regional climatic impacts of Modoki magnitude. Global and Planetary Change, Volume 172, 2019, Pages 223-241, ISSN 0921-8181. <https://doi.org/10.1016/j.gloplacha.2018.10.004>.
- Dutton, Jan. What is the Indian Ocean Dipole? Webpage. 09.02.2021. <https://www.worldclimateservice.com/2021/09/02/indian-ocean-dipole/> [Online: 20.02.2022, 21:42]
- Gore, M., B.J. Abiodun, F. Kucharski. Understanding the influence of ENSO pat- terns on drought over southern Africa using SPEEDY. Clim Dyn 54, 307–327 (2020). <https://doi.org/10.1007/s00382-019-05002-w>
- Hamouda, M.E., C. Pasquero, E. Tziperman. Decoupling of the Arctic Oscillation and North Atlantic Oscillation in a warmer climate. Nat. Clim. Chang. 11, 137–142 (2021). <https://doi.org/10.1038/s41558-020-00966-8>
- NOAA Physical Sciences Laboratory. COBE SST. Webpage. 2022. <https://www.psl.noaa.gov/data/gridded/data.cobe.html>. [Online: 17.02.2022, 13:38 PM]
- NOAA Physical Sciences Laboratory. CPC Merged Analysis of Precipitation (CMAP). Web- page. 2022. <https://psl.noaa.gov/data/gridded/data.cmap.html>. [Online: 17.02.2022, 13:39 PM]
- NOAA Physical Sciences Laboratory. NCEP/NCAR Reanalysis 1: Pressure. Webpage. 2022. <https://psl.noaa.gov/data/gridded/data.ncep.reanalysis.pressure.html>. [Online: 17.02.2022, 13:40 PM]
- NOAA CLIMATE.GOV STAFF. El Niño and La Niña: Frequently asked questions. Webpage. Updated 22.09.2021. <https://www.climate.gov/news-features/understanding-climate/el-ni%C3%B1o-and-la-ni%C3%A1a-frequently-asked-questions>. [Online: 14.02.2022, 18:20 PM]
- Snowbrains. NOAA ENSO Blog: The Rise of El Niño and La Niña. Webpage. 30.10.2020. <https://snowbrains.com/enso-blog-rise-la-nina-el-nino/>. [Online: 14.02.2022, 18:23 PM]